VII Congresso Nazionale AIDAA
15-19 September 2003 – Roma (Italy)

EXPERIMENTAL ACTIVITIES ON LIQUID PROPELLANT TURBOPUMPS AT CENTROSPAZIO

Cristina Bramanti, Angelo Cervone, Emilio Rapposelli

and

Luca d'Agostino

CENTROSPAZIO - Consorzio Pisa Ricerche
56121 Ospedaletto- Pisa, Italy
Telephone: +39 050 985072
Telefax: +39 050 974863
e-mail: c.bramanti@cpr.it

VII Congresso Nazionale AIDAA
15-19 September 2003 – Roma (Italy)

EXPERIMENTAL ACTIVITIES ON LIQUID PROPELLANT TURBOPUMPS AT CENTROSPAZIO

Cristina Bramanti[1], Angelo Cervone[‡], Emilio Rapposelli[**]

and

Luca d'Agostino[*]

CENTROSPAZIO - Consorzio Pisa Ricerche, Via Gherardesca 5, 56121 Ospedaletto- Pisa, Italy

Abstract

The present paper reviews recent experimental activities at Centrospazio on cavitation in liquid propellant turbopumps. These activities have been carried out in a dedicated, low-cost, versatile and easily instrumentable test facility, designed in 1996 under ESA (European Space Agency) funding and later refined and realized in 1999-2000 under a 1998/99 Fundamental Research contract by ASI (Italian Space Agency). The first part of the paper describes the characteristics and performance of the three alternative configurations of the facility: the CPTF (Cavitating Pump Test Facility), for general experimentation on cavitating/non-cavitating turbopumps under fluid dynamic and thermal cavitation similarity; the CPRTF (Cavitating Pump Rotordynamic Test Facility), capable of investigating rotordynamic fluid forces under forced vibration experiments on turbopump rotors of adjustable eccentricity and sub-synchronous or super-synchronous whirl speeds; and the TCT (Thermal Cavitation Tunnel), specifically designed for the investigation of 2D or 3D cavitating flows over test bodies in thermal cavitation similarity conditions. The second part of the paper presents some recent results of cavitation tests on helical inducers and hydrofoils. Future activities in this field at Centrospazio are illustrated.

Nomenclature

Latin symbols

b	blade height
c	chord length
C_p	pressure coefficient
d_S	specific diameter
f	frequency
n	number of blades
p	pressure
p_T	total pressure
P	blade pitch
$\dot{Q}$	volumetric flow rate
r	radius
Re	Reynolds number
St	Strouhal number
T	temperature
V	freestream velocity

Greek symbols

β	blade angle
ν_L	kinematic viscosity
η	efficiency
ρ	density
σ	cavitation number
ϕ	flow coefficient
ψ	head coefficient
Ω	shaft rotational speed
Ω_S	pump specific speed

Subscripts

H	hub
T	tip
V	vapor
1	pump inlet
2	pump outlet

Introduction

Cavitation, defined as "the formation of vapor bubbles in regions of low pressure within the flow field of a liquid" (Brennen, 1994), is the major source of degradation of the suction performance, reliability, power density and useful life of the turbopumps used for liquid propellant rocket engines (Stripling & Acosta, 1962). Even more importantly for space applications, cavitation can provide the necessary flow excitation, compliance and load-dependence for triggering dangerous rotordynamic and/or fluid mechanic instabilities of the turbopump (Sack & Nottage, 1965; Natanzon et al., 1974; Brennen & Acosta, 1973, 1976; Braisted & Brennen, 1980; d'Auria, d'Agostino & Brennen, 1994, 1995; d'Agostino & d'Auria 1997; d'Agostino & Venturini-Autieri 2002), or even, through the coupling with thrust

[1] Ph.D. student, Department of Aerospace Engineering, Via G. Caruso, 56126, Pisa, Italy; Research Engineer, Centrospazio - Consorzio Pisa Ricerche, 5 Via A. Gherardesca, 56121 Ospedaletto (Pisa), Italy, tel. +39 050 985097, fax. +39 050 974863, c.bramanti@cpr.it.

[‡] Ph.D. student, Department of Aerospace Engineering, Via G. Caruso, 56126, Pisa, Italy; Project Engineer, Centrospazio – Consorzio Pisa Ricerche, 5 Via A. Gherardesca, 56121 Ospedaletto (Pisa), Italy, tel. +39 050 985097, fax. +39 050 974863, a.cervone@cpr.it.

[**] Research Engineer, Centrospazio - Consorzio Pisa Ricerche, 5 Via A. Gherardesca, 56121 Ospedaletto (Pisa), Italy, tel. +39 050 985097, fax. +39 050 974863, e.rapposelli@cpr.it.

[*] Professor, Department of Aerospace Engineering, Via G. Caruso, 56122 Pisa, Italy, tel. +39 050 2217211, fax. +39 050 2217244, luca.dagostino@ing.unipi.it.

generation, of the entire propulsion system (POGO auto-oscillations of liquid propellant rockets, Rubin, 1966). In addition, in cryogenic fluids close to saturation conditions, thermodynamic phenomena associated with liquid evaporation and vapor recondensation at the cavity interface are known to represent the dominant cause of cavitation scaling effects.

Rotordynamic instabilities, the most critical of which is the development of self-sustained lateral motions (whirl) of the impeller under the action of destabilizing forces of mechanical or fluid dynamic origin, represent a crucial design aspect of turbopumps in high power density applications (Brennen 1994), because they can be responsible for very serious problems ranging from long term erosion damage to the sudden destruction of the machine (Jery et al. 1985). Rotordynamic fluid forces, when in conjunction with cavitation, significantly modify the dynamic properties of the impeller, and therefore the critical speeds of the whole machine (Franz 1989; Bhattacharyya 1994; d'Auria, d'Agostino & Brennen 1995; d'Agostino & d'Auria 1997; d'Agostino, d'Auria & Brennen 1998; d'Agostino & Venturini-Autieri 2002; Rapposelli, Falorni & d'Agostino 2002). Thus, in the presence of a sufficiently intense level of cavitation, turbopumps designed to be supercritical in non-cavitating conditions may become subcritical. Besides, cavitation also alters the orientation of the rotordynamic fluid forces, which can develop significant lateral components capable of self-sustaining the whirl motion of the impeller, thus effectively closing the loop for the onset of dangerous rotor instabilities of the pump. The recent fatigue failure of an inducer blade due to fluid dynamic instabilities of the LE-7 liquid Hydrogen turbopump (NASDA Report No. 94, May 2000, NASDA Report No. 96, June 2000) and the consequent catastrophic loss of the rocket in November 1999 dramatically confirmed the capability of fluid mechanic instabilities and rotordynamic fluid forces of critically reducing the operational life of high power density turbopumps.

On the other hand, as a rough initial approximation, the cavitating behavior of helical inducers can be related to that of a cascade of hydrofoils; therefore the first step for understanding cavitation instabilities and thermodynamic scaling effects in turbopumps is typically represented by experimentation on lifting bodies in hydrodynamic tunnels. Yet, a number of aspects of unsteady flow phenomena in cavitating turbopumps and hydrofoils, including their connection with thermal cavitation effects, are still partially understood and imperfectly predicted by theoretical means alone. Technology progress in this field must therefore heavily rely on detailed experimentation on scaled models. To this purpose Centrospazio has developed under ESA and ASI funding a low-cost, versatile and instrumentable cavitation test facility, which can be presently arranged in three alternative configurations:

- ✓ The CPTF, Cavitating Pump Test Facility, designed for general experimentation on cavitating/non-cavitating turbopumps under fluid dynamic and thermal cavitation similarity;
- ✓ The CPRTF, Cavitating Pump Rotordynamic Test Facility (Rapposelli, Cervone & d'Agostino, 2002), an upgraded version of the CPTF also capable of investigating rotordynamic fluid forces in forced vibration experiments on turbopumps with rotors of adjustable eccentricity and sub-synchronous or super-synchronous whirl speed;
- ✓ The TCT, Thermal Cavitation Tunnel (Rapposelli, Cervone, Bramanti & d'Agostino, 2002), an alternative configuration of the CPTF specifically designed for the investigation of 2D or 3D cavitating flows over test bodies in thermal similarity conditions.

Experimental Apparatus

CPTF (Cavitating Pump Test Facility)

The first configuration of the facility, the CPTF (Cavitating Pump Test Facility), is designed for conducting experiments on pumps in noncavitating/cavitating conditions under geometrical, fluid dynamic and thermal cavitation similarity, with no impeller whirl motion. It is also possible to characterize the most important cavitation instabilities of the test pump (cavitation surge and auto-oscillations, rotating cavitation, POGO instabilities). The design of the facility involved a number of technical problems and trade-offs in order to best satisfy the operational, economic and performance requirements. Priority has been given to safety and cost considerations: the facility was designed to operate at rotational speeds considerably lower than those of turbopump systems for liquid-propellant rockets using a non-dangerous fluid (water), but satisfying all of the similarity conditions essential for accurately scaling the real pump performance. This makes it possible to use the CPTF also as a "didactic" tool by graduate and undergraduate students willing to improve their experimental knowledge of turbopumps.

Another important characteristic of the CPTF is its versatility: it is capable of testing a wide variety of pumps (axial, centrifugal and mixed-flow) and can be easily reconfigured to carry out investigations on a large number of fluid dynamic phenomena relevant to turbopump operation (rotating cavitation, POGO instabilities, cavitation noise, tip leakage, vortex shedding, blade flutter, transient phenomena, liquid quality effects, flow visualization, etc.).

The architecture of the CPTF, schematically illustrated in Figure 1, consists of a closed water loop comprising the necessary equipment for controlling the operational parameters of the pump, and an instrumented test section where the pump itself is located. Figure 1 also shows a picture of the facility.

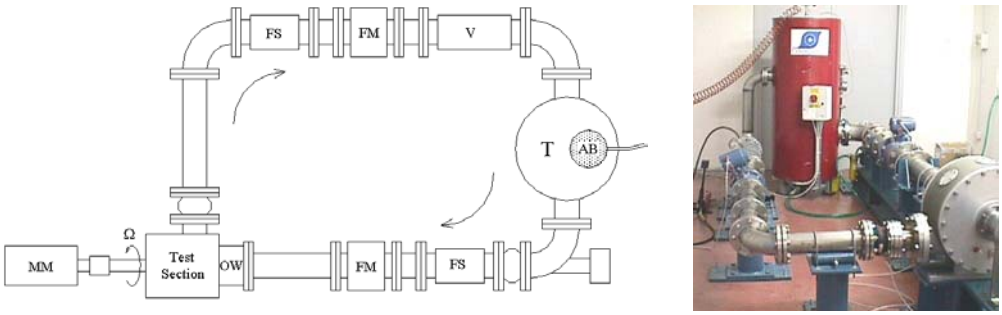

Figure 1 – Schematic of the CPTF (left) and a picture of the water loop (right).

The loop is made of flanged stainless steel (AISI 316) pipes, with an internal pipe diameter of 6" on the suction line and 4" on the discharge line; the active portion of the facility (motors, mechanical transmissions, test section and inlet line) is mounted on a very stiff carbon-steel beam structure.

Referring to Figure1, the main components of the CPTF are:

- ✓ The 0.5 m^3 stainless steel tank (T) used to regulate water properties (temperature and pressure) and to uncouple the inlet/outlet volume fluctuations generated by cavitation in the pump. To this purpose the tank makes use of a 5 kW electrical resistance and a 40 liters air-bag (AB) connected to an air compressor or a water ring vacuum pump.
- ✓ The valve (V), which generates the adjustable pressure drop necessary to load the pump and separates the suction and discharge lines. The particular valve used, called "Silent Throttle Valve", creates a distributed loss capable of yielding large pressure drops without inducing unsteady cavitation, which would generate unwanted dynamic noise and additional cavitation nuclei (microbubbles) in the working fluid.
- ✓ The electromagnetic flowmeters (FM), one on the suction line and one on the discharge line, used to measure flow rate and velocity.
- ✓ The flow straighteners (FS), honeycomb-filled pipe sections that drastically reduce the flow turbulence and rotation for better operation of the flowmeters and providing more regular flow conditions at the pump inlet.
- ✓ The main motor (MM), a 6-pole, 30 kW, brushless motor driven by power electronics capable of controlling one or more motors in angular position or speed. The motor is connected to the pump by a omokinetic, torsionally stiff coupling, in order to accommodate the misalignments due to mounting or manufacturing errors.
- ✓ The test section (Figure 2), that is the "housing" where the test pump is mounted together with its volute. The dimensions and interfaces of the test section have been chosen in order to house a large number of different pumps, in particular the new evolution (called "Mark 2") of the liquid oxygen turbopump of the Ariane 5 "Vulcain" engine, used as the reference pump for the design of the facility. The inlet of the test section (OW) consists of a transparent tube with plane external surfaces, allowing for optical visualization of the flow into the axial stage of the test pump.

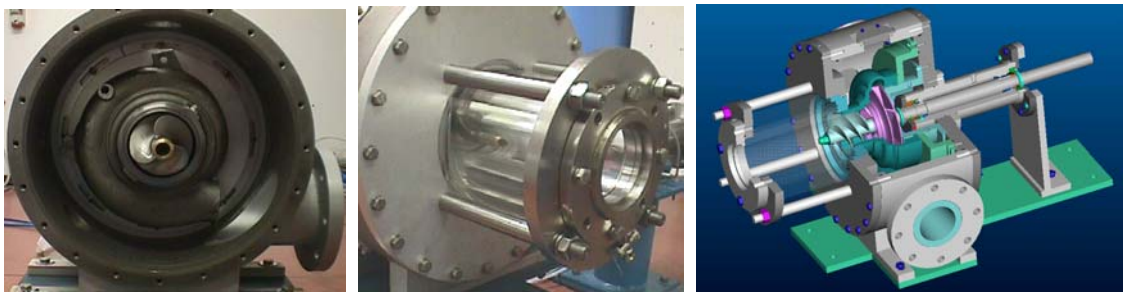

Figure 2 – The test section of the CPTF: the internal of the housing with the pump volute (left), the transparent inlet section (center), and a drawing of the test section assembly (right).

Several kinds of pressure transducers are used to experimentally characterize the cavitating/noncavitating behavior of the pump: in particular, absolute transducers monitor the suction pressure at the inlet of the pump; differential transducers provide the information on the pressure rise generated by the machine; piezoelectric transducers can be mounted circumferentially, upstream or downstream of the pump, in order to analyze the frequency spectrum of the pressure fluctuations caused by cavitation instabilities.

Operational envelope and scaling characteristics of the CPTF

The nominal operational parameters of the CPTF are listed in Table 1. Figure 3 shows the operational envelope of the facility in the $\Omega_S - d_S$ plane (i.e., the range of values of specific speed and specific diameter for which pumps can be tested in the facility).

Internal diameter of the pump housing	500 mm
Maximum tip radius of test inducer	82 mm
Maximum tip radius of test impeller	150 mm
Suction line pipes I.D.	6”
Discharge line pipes I.D.	4”
Working fluid	water
Maximum pump pressure rise	10 atm
Maximum absolute pressure at pump inlet	6 atm
Minimum absolute pressure at pump inlet	0.1 atm
Maximum flow rate	0.1 m^3/sec
Maximum working temperature	100°C
Maximum main motor rotating speed	3000 rpm
Maximum main motor power	30 kW
Maximum main motor torque	100 Nm

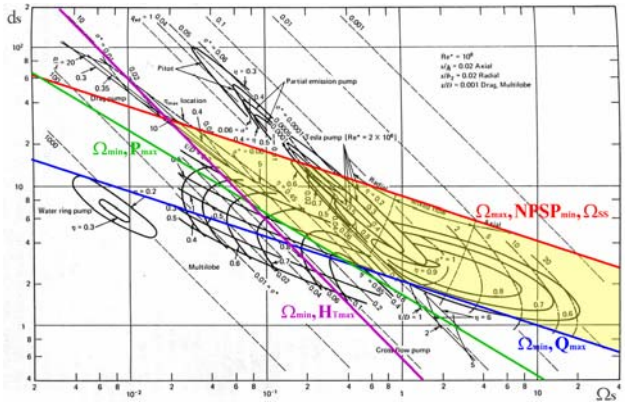

Table 1 (left) – CPTF operational characteristics.
Figure 3 (right) **–** CPTF operational envelope: all pumps whose nominal values of the specific speed and diameter fall inside the highlighted area bounded by the constraints in the figure can be tested under fluid dynamic similarity conditions in the CPTF.

Even if pumps used in space applications typically operate at quite higher velocity and power levels, the CPTF can accurately simulate their performance by means of the well known scaling criteria for geometrical and fluid dynamic similarity. The possible occurrence of thermal cavitation introduces a second important similarity criterion to be matched, especially when the real pump operates with a cryogenic fluid. In this case the saturated vapor density is relatively high and can decrease significantly during the cavity growth, thereby appreciably reducing the driving force for the occurrence of cavitation and delaying its development (Brennen 1994). As shown in Figure 4, in order to correctly scale cryogenic fluids in water in the CPTF it is necessary to work at suitably elevated temperatures depending on the sizes and speeds of the turbopump and its test model. On the other hand, thermal scaling in water of many kinds of less volatile storable hydrocarbons would nominally require reduced flow temperatures, although in practice room temperature water is sufficient since it leads to negligible thermal cavitation effects.

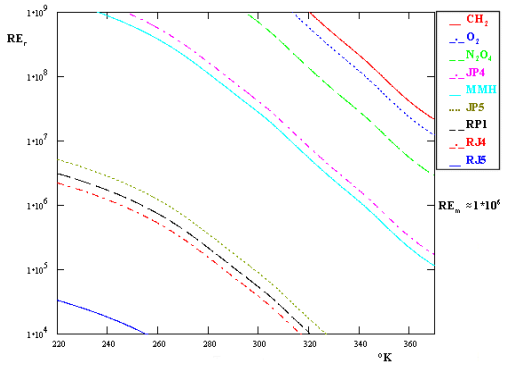

Figure 4 - Equivalent water temperature in the CPTF for scaling a pump operating with different propellants and Reynolds numbers. The Reynolds number of the pump in the CPTF is $\mathrm{Re} = \boldsymbol{\Omega} r_T^2 / \boldsymbol{\nu}_L = 10^6$.

CPRTF (Cavitating Pump Rotordynamic Test Facility)

The analysis of whirl phenomena and rotordynamic instabilities can conceivably be accomplished either in a free or in a forced vibration experiment. Actual rotordynamic destabilization of a turbopump according to the former approach is not practically feasible in a laboratory environment (apart from safety and economic considerations) due to the large power densities that would be required and the impossibility of simultaneously scaling geometric, kinematic, structural and fluid properties of the turbomachine to preserve structural and fluid dynamic similarity. It is therefore necessary to experimentally reproduce the whirl motion under carefully controlled conditions and measure the impeller forces in a forced vibration experiment.

As a result of these considerations, the CPRTF configuration of the facility is obtained by introducing a mechanism for imparting the test pump a “forced” whirl motion with given eccentricity, constant during each experiment but adjustable from one experiment to another. Table 2 lists the main operational characteristics of CPRTF, while Figure 5 shows a drawing of its test section.

Maximum whirl rotating speed	3000 rpm
Maximum auxiliary motor power	5 kW
Maximum auxiliary motor torque	20 Nm
Adjustable whirl eccentricity	0 ÷ 2 mm
Nominal suspended mass	4 kg
Maximum dynamometer loads:	
lateral	2400 N
axial	15000 N
bending	1400 N
torque	400 N

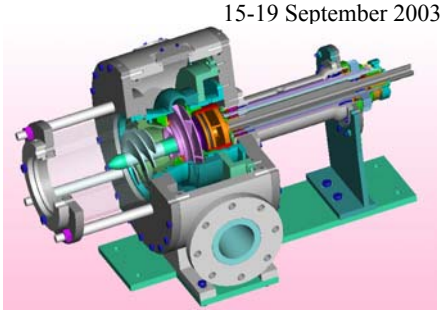

Table 2 (left) – CPRTF operational characteristics.
Figure 5 (right) **–** The test section assembly of the CPRTF with the rotating dynamometer (orange component).

The main components of the CPRTF configuration are:

- ✓ The eccentric drive mechanism, consisting of the combination of two cylinders, each with 1 mm fixed eccentricity. The inner cylinder internally supports the pump shaft, the outer one is externally supported by the pump stator. Before each run the relative angle of the two eccentricities can be finely adjusted and fixed between 0° and 180°, realizing a total shaft eccentricity varying from 0 to 2 mm.
- ✓ The auxiliary motor, a 6-poles, 5.6 kW, brushless motors, which drives the eccentric mechanism. The motor is controlled by its power electronics in angular position and velocity with reference to the main motor, in order to retain a specified and commensurable velocity ratio ω/Ω and realize periodic rotation and whirl configurations at the beginning and the end of each test period.
- ✓ The rotating dynamometer (Figure 6), realized in just one piece of phase hardening steel AISI PH 17-4. It comprises two flanges connected by four square pillars acting as flexing elements, whose deformation is sensed by 40 semiconductor strain gauges arranged in 10 full bridges, which provide 10 redundant measurements of the 6 forces and moments acting on the impeller.
- ✓ The slip rings assembly, necessary to realize with accuracy and stability the electrical connections between the instrumented rotor (rotating dynamometer or other impeller-mounted sensors) and the stationary electronics (exciters, amplifiers and data acquisition).

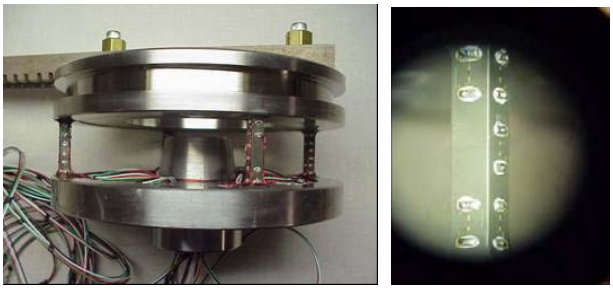

Figure 6 – The rotating dynamometer (left) and a close view of the strain gauges arrangement on one post (right).

TCT (Thermal Cavitation Tunnel)

This configuration is specifically designed for analyzing 2D or 3D cavitating flows over test bodies, using the pump simply to generate the required mass flow. The tunnel is mounted in the suction line of the facility and the geometry of its inlet, test and outlet sections has been chosen in order to generate a sufficiently fast and uniform flow on the test bodies, with an adequate pressure recovery in the diffuser for suppressing cavitation in the pump. Figure 7 shows two pictures of the facility in the TCT configuration and of the tunnel test section.

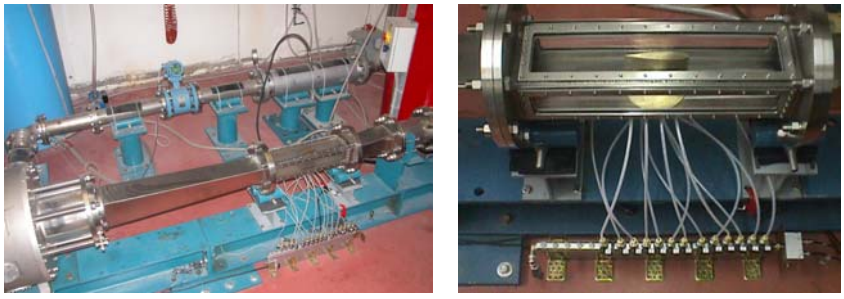

Figure 7 – The Thermal Cavitation Tunnel**.** The entire facility (left) and its test section (right).

The test body used for actual experimentation is a NACA 0015 hydrofoil with 115mm chord and 80mm span length, mounted on a blind panel on the bottom of the rectangular test section (120x80x500mm). Optical access is allowed through three large plexiglas windows located on the lateral and top sides of the test section.

Figure 8 shows a schematic of the test section, with the hydrofoil instrumented with 12 pressure taps, 10 on the suction side and 2 on the pressure side. Two sets of three taps are located on the bottom panel both upstream and downstream of the test section to monitor the inlet/outlet pressure. The incidence angle can be manually adjusted as necessary for the specific experiment. The tunnel maximum velocity is 8 m/s and the Reynolds number ($\mathrm{Re} = c \cdot V / \upsilon_L$) can be maintained higher than $5 \cdot 10^5$ during the tests.

Dimensions of test section	120x80 mm
Total length of tunnel	1709 mm
Test hydrofoil	NACA 0015
Hydrofoil chord	115 mm
N° of total pressure taps	12
N° of pressure taps on suction side	10
N° of pressure taps on pressure side	2
Maximum freestream speed	8 m/sec

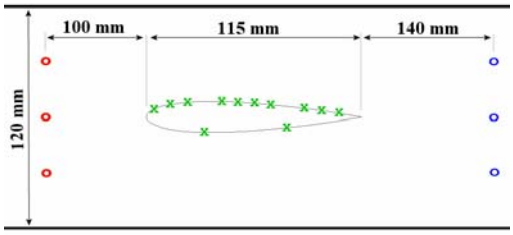

Table 3 (left) – TCT operational characteristics.
Figure 8 (right) – Schematic of the test section with the NACA 0015 hydrofoil and the locations of the pressure taps on the hydrofoil surface (x), at the section inlet (o) and outlet (o).

Experimental Activity

Cavitation Experiments on Liquid Propellant Turbopumps

A first set of experimental tests has been conducted for validating the CPTF; the pump used in this phase (Figure 9 left) is a commercial one, whose main characteristics are reported in Table 4. In particular, Figure 9 (right) shows the characteristic curves of the complete pump (axial inducer and centrifugal impeller), namely the behavior of the work coefficient $\psi = \Delta p_t \big/ \rho \Omega^2 \mathrm{r}_{T2}^2$ and the efficiency η as functions of the flow coefficient $\phi = \dot{Q} \big/ 2\pi b_2 \Omega r_{T2}^2$.

Test pump characteristics	*inducer*	*impeller*	*Ind+imp*
Inlet tip radius r_T	60 mm	60 mm	
Outlet tip radius r_{T2}		107 mm	
Inlet hub radius r_H	19 mm	19 mm	
Outlet blade width b_2		22 mm	
Number of blades n	3	6	
Tip angle β_T	18°		
Pitch P	110 mm		
Nominal specific speed Ω_S	2.05	1.3	1.7
Nominal specific diameter d_S	2.33	2.15	1.78

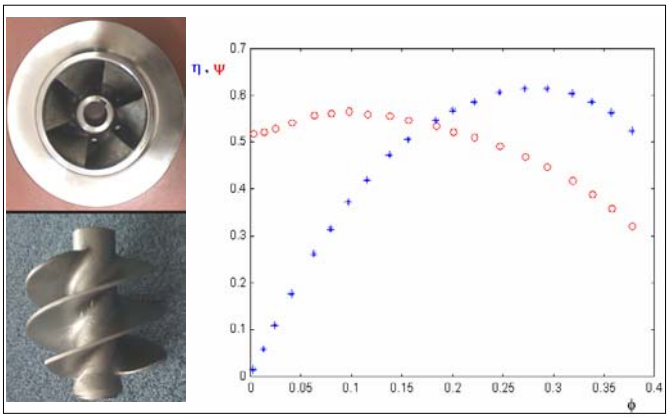

Table 4 (left) **-** Characteristics of the pump used for the validation of the CPTF
Figure 9 (right) - Axial inducer and impeller of the test pump used for CPTF validation (left). Head coefficient (circles) and efficiency (crosses) of the CPTF test pump (impeller with inducer) as functions of the flow coefficient (right).

Figure10 (left) shows the suction characteristics of the three-bladed helical inducer coupled to the centrifugal impeller at room temperature for different values of the flow coefficient ϕ. It can be observed that the decrease of the flow coefficient ϕ causes both the decrease of the cavitation breakdown number and the increase of the work coefficient. This behavior is different if the inducer is tested alone (Figure 11 left): here, in fact, the decrease of the flow coefficient ϕ produces both the increase of the cavitation breakdown number as well as of the work coefficient. Figures 10 (right) and 11 (right) illustrate the influence of the thermal cavitation effects on the suction performance of the reference inducer with and without the centrifugal impeller, respectively. As expected, at higher values of the water temperature the cavitation breakdown occurs at lower pressures and the work coefficient increases slightly. At higher temperatures, as previously pointed out, the evaporation of the liquid in growing bubble cools the interface, reducing the vapor pressure under the unperturbed saturation value (thermal cavitation effect). Two different conditions of the cavitating flow in the test inducer are illustrated in Figure 12.

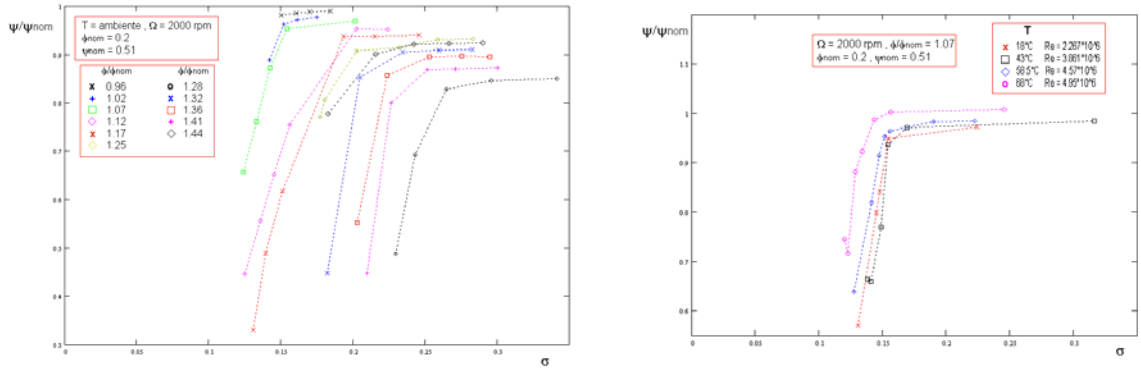

Figure 10 - Suction characteristics of the three-bladed helical inducer ($\beta_T = 18°$, $r_T = 60\ mm$, $r_H = 22\ mm$) coupled to the centrifugal impeller ($b_2 = 22\ mm$, $r_{T1} = 60$ mm , $r_{T2} = 107$ mm) in water for several flow coefficients at room temperature (left) and various temperatures (right).

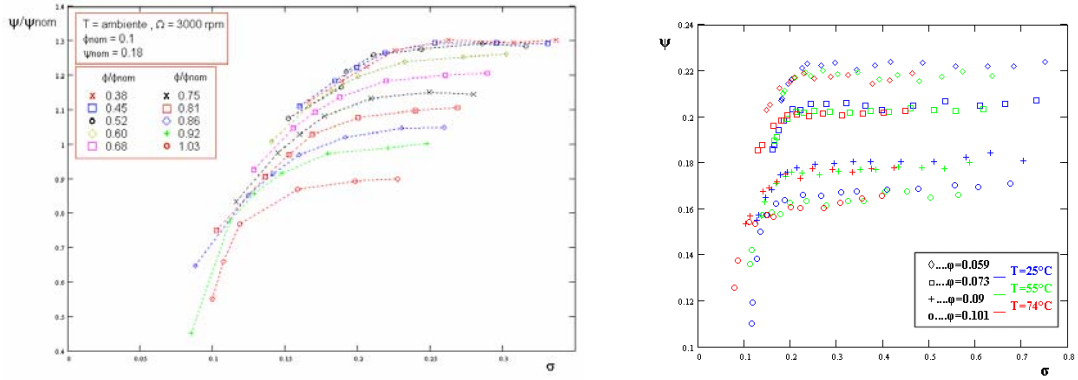

Figure 11 - Suction characteristics of the three-bladed helical inducer ($\beta_T = 18°$, $r_T = 60\ mm$, $r_H = 22\ mm$) in water at Re = $\Omega r_T^2 / \nu_L = 10^6$ for several flow coefficients at room temperature (left) and various temperatures (right).

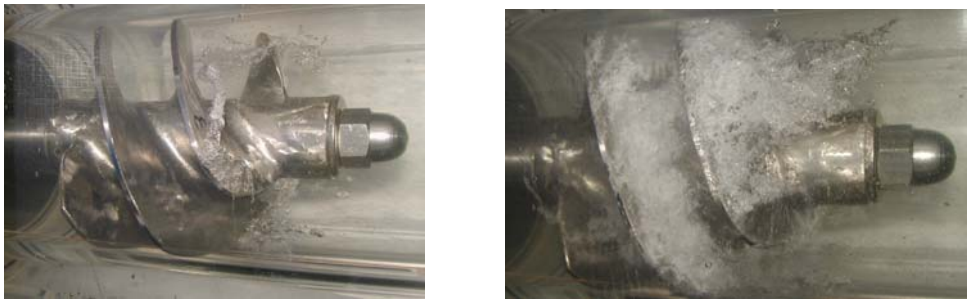

Figure 12 - Two examples of cavitation in three-bladed helical inducer ($\beta_T = 18°$, $r_T = 60\ mm$, $r_H = 22\ mm$) at room water temperature and cavitation numbers $\sigma = 0.369$ (left) and $\sigma = 0.116$ (right).

As previously mentioned, the experimental characterization of the fluid mechanic instabilities caused by cavitation is essential in order to avoid the onset of the dangerous regimes of the turbopump and to allow for a better understanding of the phenomena involved, which can lead to the rapid degradation of the turbomachinery performance. To this purpose, a number of experiments have been carried out in the CPTF in order to determine the fluctuations of the inducer inlet pressure and flow rate and to detect the instabilities connected to cavitation.

Figure 13 shows the frequency spectra of the flow pressure just upstream of the inducer inlet section as a function of the cavitation number σ at room temperature and at two different flow coefficients ϕ. At lower flow coefficients (Figure 13, left) only low frequencies around 3-4 Hz (typical of cavitation auto-oscillations or cavitation surge) dominate (Furukawa, Ishizaka & Watanabe, 2001; Mark, Duttweiler & Brennen, 2001). This form of instability is associated with a positive slope of the pump head rise/flow rate curve, when the inducer is more heavily loaded (Figure 13, down). At higher flow coefficients (Figure 13 right) the oscillations occur at a frequency equal to about 50% of the inducer rotational speed: they are probably due to the occurrence of rotating cavitation (Fujii, Azuma, Yoshida, Tsujimoto, Horiguchi & Watanabe, 2002), associated to a negative slope of the pump head rise/flow rate curve (Figure 13, down).

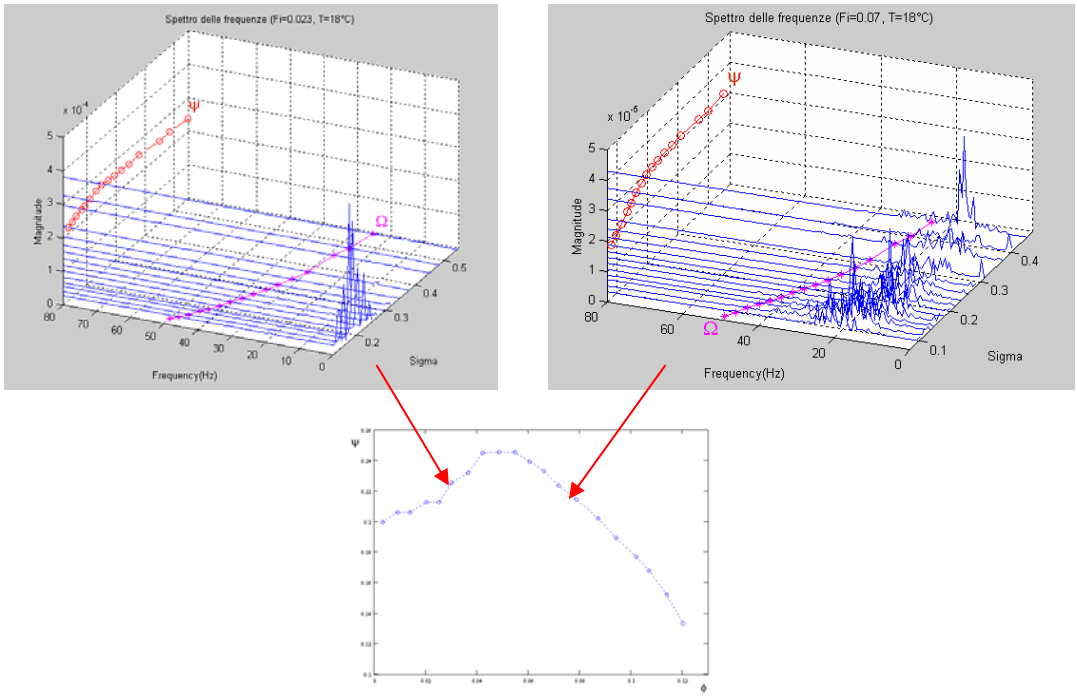

Figure 13 - Frequency spectra of the inlet pressure of the inducer ($\beta_T = 18°$, $r_T = 60\ mm$, $r_H = 22\ mm$) as a function of the cavitation number σ at room temperature and flow coefficients $\phi = 0.023$ (left) and $\phi = 0.07$ (right). Head coefficient of the three-bladed helical inducer at room water temperature (down).

Cavitation Experiments on NACA 0015 Hydrofoil

The extensive experimentation on thermal cavitation effects on a NACA 0015 hydrofoil presented in this section has been carried out in the TCT (Thermal Cavitation Tunnel), the last alternative configuration of the facility. Figure 14 shows the pressure coefficient for each pressure tap located on the suction side of the hydrofoil in noncavitating (left) and inertial/thermal cavitating (right) conditions at constant tunnel velocity, water temperature, foil incidence angle and cavitation number $\sigma = (p_1 - p_V) / \frac{1}{2}\rho V^2$. Figure 14 (left) confirms that the lateral constraints to the flow cause significant deviations from the surface pressure distribution in unconstrained noncavitating flow. These deviations arise because blockage generated by the occurrence of cavitation increases the dynamic pressure of the flow, and therefore also the hydrofoil forces and moments at a given incidence angle. In the same figure the pressure distribution obtained from a fully-wetted CFD simulation of the free-space hydrofoil at 8° incidence angle is compared with the experimental results in order to illustrate their good agreement.

In Figure 14 (right) the pressure coefficient profile is presented for 5° flow incidence at three different water temperatures and the same cavitation number. As previously pointed out, thermal effects significantly modify the surface pressure distribution, shortening the length of the cavitating region.

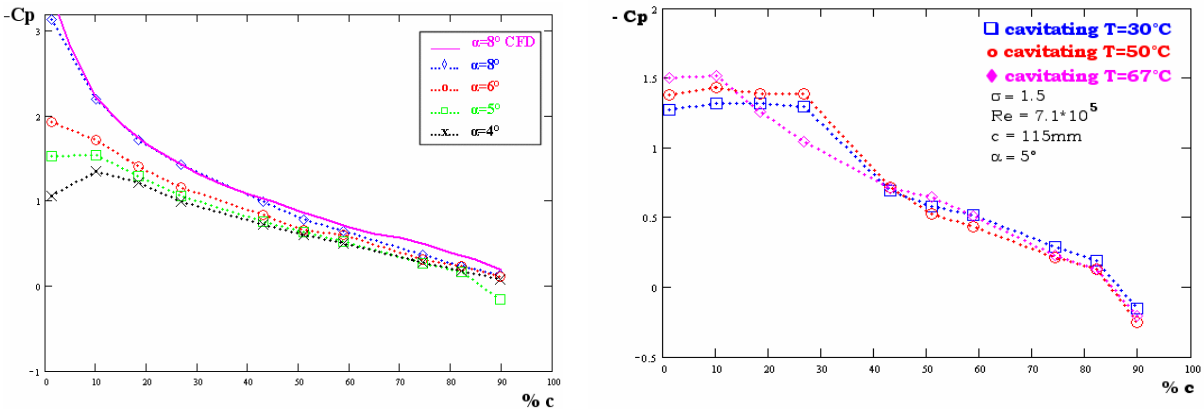

Figure 14 - Pressure coefficient on the suction side of the NACA 0015 hydrofoil in noncavitating conditions for various incidence angles α at room water temperature. CFD simulation of the hydrofoil pressure distribution at 8° incidence angle and room water temperature (solid line) (left). Influence of thermal cavitation effects on surface pressure distribution on the NACA 0015 hydrofoil for several water temperatures T at 5 ° incidence angle and constant cavitation number σ (right).

Additional tests have been carried out with the aim of determining the behavior of the cavity length and oscillations at different incidence angles, cavitation numbers and freestream temperature. The cavity length has been calculated, with a maximum estimated error of 4% of the chord length, by taking pictures (30 frames for 1 second) of the cavitating hydrofoil. In particular, Figure 15 shows the maximum and minimum cavity lengths for 8° incidence angle at room water temperature (left) and at 50 °C and 70 °C (right). Simultaneously, frequency spectra of the upstream pressure have also been measured in each flow condition and temperature (figure 16). From the analysis of Figures 15 and 16 it is possible to obtain a good qualitative indication of cavitation behavior on the hydrofoil at different cavitation numbers and to recognize three different regimes of cavitation, corresponding to different ranges of values of σ:

- Supercavitation ($\sigma < 1.3$): both the minimum and maximum cavity lengths are larger than the chord length. There are practically no cavity oscillations and therefore the frequency spectrum is almost flat.

- Bubble+cloud cavitation ($1.3<\sigma<2$): the flow pictures show the occurrence of an initial zone of bubbly cavitation, followed by a second zone where the bubbles coalesce and strong cloud cavitation oscillations are observed. The frequency of these oscillations is almost constant at different cavitation numbers, with a Strouhal number ($St = f \cdot c / V$) of about 0.2.

- Bubble cavitation ($\sigma >2.1$): after a short transition zone, cloud cavitation disappears. Only the traveling bubble cavitation zone remains, with drastically reduced pressure oscillations (flat frequency spectrum).

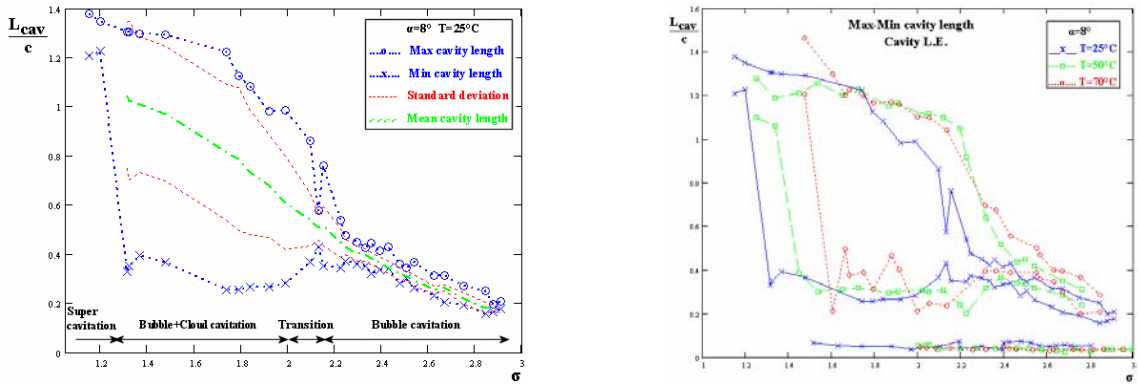

Figure 15 – Mean length and oscillation of the cavity on a NACA 0015 hydrofoil at 8° incidence angle and room water temperature as functions of the cavitation number σ (left). Origin and oscillation of the cavity on the same hydrofoil at 8° incidence angle as functions of the cavitation number σ for three different water temperatures T (right).

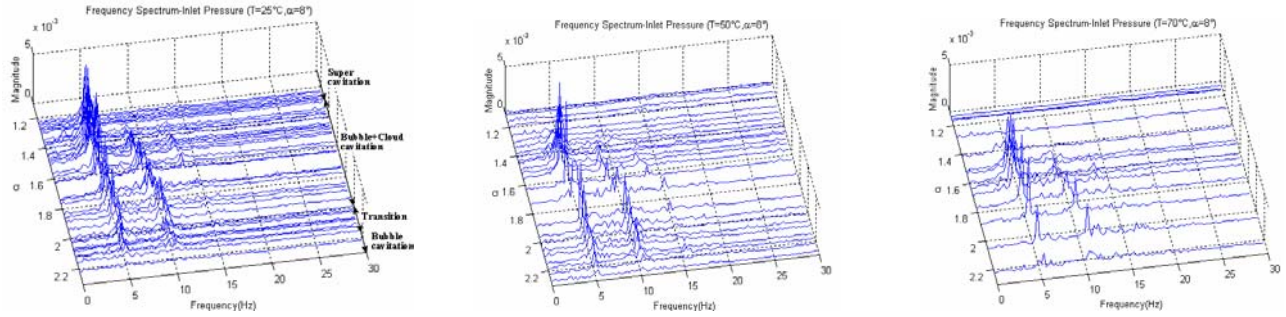

Figure 16 - Frequency spectra of the upstream pressure on a NACA 0015 hydrofoil at 8° incidence angle and room water temperature (left), 50°C (centre), and 70°C (right).

The different appearance of the cavitation at various freestream temperatures is well illustrated in Figure 17: at higher temperatures bubbles are smaller and tend to coalesce more easily, resulting in a narrower and less defined "bubble zone" compared to the "cloud zone".

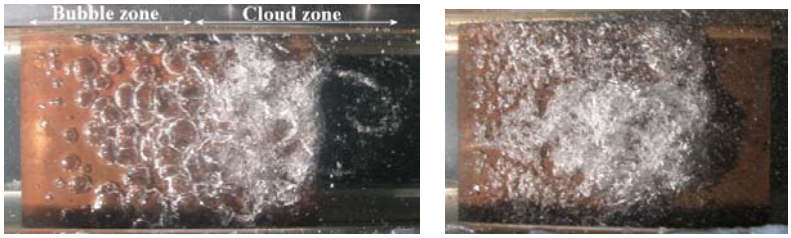

Figure 17 - Typical cavitation appearance in "Bubble+Cloud" case ($\alpha = 4°, \sigma = 1.25, T = 25°C$) (left). Cavitation appearance at higher freestream temperature ($\alpha = 8°, \sigma = 2, T = 70°C$) (right).

The experimental tests also demonstrated that at higher temperatures:

- the supercavitation zone begins at higher values of σ;
- the bubble+cloud cavitation zone tends to spread over a wider range of cavitation numbers and to begin at higher values of σ;
- cavitation bubbles become smaller and tend to coalesce;
- the cavity becomes thicker and longer.

Conclusions and Future Activities

In the last years Centrospazio has carried out an intensive experimental activity on turbopumps used for space propulsion applications, with particular attention to cavitation and related instabilities. This activity has been made possible through the realization of a low-cost, versatile and instrumentable facility, with three main available configurations: the CPTF (Cavitating Pump Test Facility), for general experimentation on cavitating/non-cavitating turbopumps; the CPRTF (Cavitating Pump Rotordynamic Test Facility), capable of investigating rotordynamic fluid forces in forced vibration experiments on turbopumps with rotors of adjustable eccentricity and sub-synchronous or super-synchronous whirl speed; and the TCT (Thermal Cavitation Tunnel), specifically designed for the investigation of 2D or 3D cavitating flows over test bodies in thermal similarity conditions. The facility has been validated by a set of experiments on a commercial pump constituted by a three-bladed axial inducer and a six-bladed centrifugal impeller. In TCT configuration, extensive experimentation has been carried out on a NACA 0015 hydrofoil, in order to characterize the pressure distribution in cavitating/noncavitating conditions, the behavior of cavity length and oscillations, and the thermal effects on cavitation and cavity oscillations.

According to the original design requirements, the facility demonstrated to be readily adaptable for carrying out a wide range of fluid dynamic tests relevant to the characterization of high performance turbopumps in similarity conditions accurately representative of full-scale operation.

The main activities planned for the near future are:

- the experimental characterization of the performance of two new inducers (Figure 18) in noncavitating and thermal/inertial cavitating conditions;

- the measurement of the steady and unsteady rotordynamic forces exerted by the flow on whirling impellers of cavitating/noncavitating turbopumps using the CPRTF;

- the measurement and analysis of dynamic tests and frequency spectra in order to investigate the nature and development of cavitation-induced instabilities;

- the experimental characterization of cavitation damage and erosion on metallic and surface-coated test bodies and turbopumps;

- the upgrading of the optical instrumentation for flow visualization and measurement.

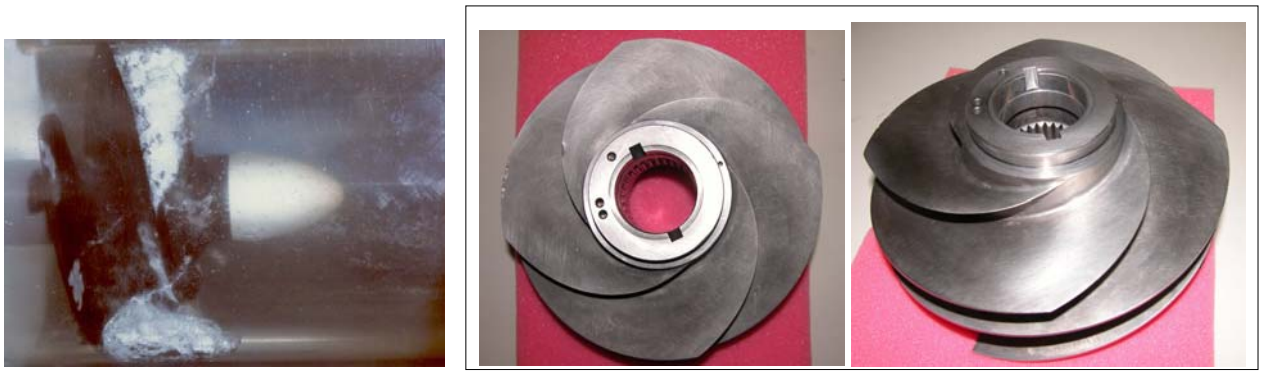

Figure 18 - Cavitation in a three-bladed helical inducer ($\beta_T = 9°$, $r_T = 80\ mm$, $r_H = 22\ mm$) at room water temperature (left). The four-bladed helical inducer of the Vulcain Engine LOX turbopump (right).

Acknowledgments

The design of the facility has been supported by the European Space Agency under the FESTIP-1 contract No. 11.482/95/NL/FG and its realization by the Agenzia Spaziale Italiana under the 1998 and 1999 contracts for fundamental research. The authors would like to acknowledge the help of the students F. d'Auria, S. Bondi, D. Mazzini, R. Menoni, L. Vigiani, A. Milani, N. Saggini and R. Testa, who participated to the design of the facility, and express their gratitude to Profs. Mariano Andrenucci and Renzo Lazzeretti of the Dipartimento di Ingegneria Aerospaziale, Università degli Studi di Pisa, Pisa, Italy, for their constant and friendly encouragement.

References

Bhattacharyya A., 1994, "Internal Flows and Force Matrices in Axial Flow Inducers", *Ph. D. thesis, Div. Eng. & Appl. Science, Caltech*, Pasadena, CA, USA.

Braisted D.M. and Brennen C.E., 1980, "Auto-Oscillation of Cavitating Inducers", *Polyphase Flow and Transport Technology, ed. R.A. Bajura,* ASME Publ., New York, pp. 157-166.

Brennen C.E., 1994, "Hydrodynamics of Pumps", *Concepts ETI, Inc*. and *Oxford University Press*.

Brennen C.E. and Acosta A.J., 1976, "The Dynamic Transfer Function for a Cavitating Inducer", *ASME J. Fluids Eng*., Vol. 98, pp. 182-191.

Brennen C.E. and Acosta A.J., 1973, "Theoretical, Quasi-Static Analysis of Cavitation Compliance in Turbopumps", *J. Spacecrafts & Rockets*, Vol. 10, No. 3, pp. 175-180.

d'Agostino L., & Venturini-Autieri M., 2002, "Three-Dimensional Analysis of Rotordynamic Fluid Forces on Whirling and Cavitating Finite-Length Inducers", *9th Int. Symp. on Transport Phenomena and Dynamics of Rotating Machinery (ISROMAC-9),* Honolulu, HI, USA, February 10-14.

d'Agostino L. & d'Auria F., 1997, "Three-Dimensional Analysis of Rotordynamic Forces on Whirling and Cavitating Inducers", *ASME FED Summer Meeting*, Vancouver, BC, Canada, June 22-26.

d'Agostino L., d'Auria F. & Brennen C.E., 1998, "A Three-Dimensional Analysis of Rotordynamic Forces on Whirling and Cavitating Helical Inducers", *ASME J. of Fluids Eng.,* Vol. 120, pp. 698-704.

d'Auria F., d'Agostino L. & Brennen C.E., 1994, "Linearized Dynamics of Bubbly and Cavitating Flows in Cylindrical Ducts", *ASME FED Summer Meeting, Incline Village*, NV, USA, June 19-23.

d'Auria F., d'Agostino L. & Brennen C.E., 1995, "Bubble Dynamic Effects on the Rotordynamic Forces in Cavitating Inducers", *ASME FED Summer Meeting*, Hilton Island, SC, USA, August 13-18.

Franz R. et al., 1989, "The Rotordynamic Forces on a Centrifugal Pump Impeller in the Presence of Cavitation", *ASME FED-81*, pp. 205-212.

Fujii A., Azuma S., Yoshida Y., TsujimotoY., Horiguchi H. & Watanabe S., 2002, "Higher Order Rotating Cavitation in an Inducer", *9th of Int. Symp. on Transport Phenomena and Dynamic of Rotating Machinery,* Honolulu, HI, USA, Feb. 10-14.

Furukawa A., Ishizaka K., Watanabe S., 2001, "Experimental Estimate of Helical Inducer Blade Forces in Cavitation Surge Condition", *CAV2001, International Symposium on Cavitation,* Pasadena, California USA, June 20-23.

Jery B. et al., 1985, "Forces on Centrifugal Pump Impellers", *2nd Int. Pump Symp*., Houston, TX, USA, April 29-May 2, 1985.

Mark E. Duttweiler 1 & Brennen C.E., 2001, "Surge Instabily on a Cavitating Propeller", *CAV2001, International Symposium on Cavitation,* Pasadena, California USA, June 20-23.

NASDA, 2000a, b, *Report No. 94, No. 96*, May and June 2000.

Natanzon M.S. el al., 1974, "Experimental Investigation of Cavitation Induced Oscillations of Helical Inducers", *Fluid Mech. Soviet Res*., Vol. 3 No. 1, pp.38-45.

Rapposelli E., Falorni R. & d'Agostino L., 2002, "Two-Phase and Inertial Effects on the Rotordynamic Forces in Whirling Journal Bearings", *Proc. 2002 ASME FED Summer Meeting*, Montreal, Quebec, Canada, July 14-18.

Rapposelli E., Cervone A. & d'Agostino L., 2002, "A New Cavitating Pump Rotordynamic Test Facility", *AIAA Paper 2002-4285, 38th AIAA/ASME/SAE/ASEE Joint Propulsion Conference*, Indianapolis, IN, USA, July 8-11.

Rapposelli E., Cervone A., Bramanti C. & d'Agostino L., 2002, "A New Cavitation Test Facility at Centrospazio", *4th International Conference on Launcher Technology*, Liege, Belgium, December 3-6.

Rapposelli E., Cervone A., Bramanti C. & d'Agostino L., 2002, "Thermal Cavitation Experiments on a NACA 0015 Hydrofoil", *4th ASME_JSME Joint Fluids Engineering Conference*, Honolulu, USA, July 6-10.

Rubin S., 1966, "Longitudinal Instability of Liquid Rockets due to Propulsion Feedback (POGO)", *J. of Spacecraft and Rockets*, Vol.3, No. 8, pp.1188-1195.

Sack L.E. and Nottage H.B., 1965, "System Oscillations Associated to Cavitating Inducers", *ASME J. Basic Eng*., Vol. 87, pp. 917-924.

Stripling L.B. and Acosta A.J., 1962, "Cavitation in Turbopumps – Part 1", *ASME J. Basic Eng*., Vol. 84, pp. 326-338.